

THE ROLE OF ELECTRON CAPTURES IN CHANDRASEKHAR MASS MODELS FOR TYPE IA SUPERNOVAE

Franziska Brachwitz¹, David J. Dean², W. Raphael Hix^{2,3}, Koichi Iwamoto⁴, Karlheinz Langanke⁶, Gabriel Martínez-Pinedo⁶, Ken’ichi Nomoto^{5,7}, Michael R. Strayer², Friedrich-K. Thielemann^{1,2}, Hideyuki Umeda⁷

ABSTRACT

The Chandrasekhar mass model for Type Ia Supernovae (SNe Ia) has received increasing support from recent comparisons of observations with light curve predictions and modeling of synthetic spectra. It explains SN Ia events via thermonuclear explosions of accreting white dwarfs in binary stellar systems, being caused by central carbon ignition when the white dwarf approaches the Chandrasekhar mass. As the electron gas in white dwarfs is degenerate, characterized by high Fermi energies for the high density regions in the center, electron capture on intermediate mass and Fe-group nuclei plays an important role in explosive burning. Electron capture affects the central electron fraction Y_e , which determines the composition of the ejecta from such explosions. Up to the present, astrophysical tabulations based on shell model matrix elements were only available for light nuclei in the sd-shell. Recently new Shell Model Monte Carlo (SMMC) and large-scale shell model diagonalization calculations have also been performed for pf-shell nuclei. These lead in general to a reduction of electron capture rates in comparison with previous, more phenomenological, approaches. Making use of these new shell model based rates, we present the first results for the composition of Fe-group nuclei produced in the central regions of SNe Ia and possible changes in the constraints on model parameters like ignition densities ρ_{ign} and burning front speeds v_{def} .

¹Department of Physics and Astronomy, University of Basel, CH-4056 Basel, Switzerland

²Physics Division, Oak Ridge National Laboratory, Oak Ridge, TN 37831-4576, USA

³Department of Physics and Astronomy, University of Tennessee, Knoxville, TN 37996-1200, USA

⁴Department of Physics, Nihon University, Tokyo 101-8308, Japan

⁵Department of Astronomy, University of Tokyo, Tokyo 113-0033, Japan

⁶Institute of Physics & Astronomy, University of Aarhus, DK-8000 Aarhus C, Denmark

⁷Research Center for the Early Universe, School of Science, University of Tokyo, Tokyo 113-0033, Japan

Subject headings: nuclear reactions, nucleosynthesis, abundances; supernovae: general; white dwarfs

1. Introduction

Electron capture is an important phenomenon in the late phases of stellar evolution, during stellar collapse, and in explosive events like Type I supernovae (SNe Ia), Type II supernovae (SNe II), and possibly in X-ray bursts (rp-process). Its takes place in high density matter, where the Fermi energy of a degenerate electron gas is sufficiently large to overcome the energy thresholds given by the negative Q-values of such reactions. The Fermi energy exceeds a fraction of an MeV in late burning stages, allowing electron capture initially only for a few selected nuclei like ^{33}S and ^{35}Cl (with small energy thresholds of 0.247 MeV or ^{35}Cl , respectively), and goes beyond an MeV during Fe-core collapse or SNe Ia explosions.

In the following we discuss the effects of electron capture on nuclei during the flame propagation in SNe Ia. There are strong observational and theoretical indications that SNe Ia (a classification based on the absence of hydrogen lines and the presence of a specific SiII line in their spectra) are thermonuclear explosions of accreting white dwarfs (e.g., Nomoto et al. 1994; Wheeler et al. 1995; Höflich & Khokhlov 1996; Nomoto, Iwamoto, & Kishimoto 1997; Nomoto et al. 1997; Höflich et al. 1997; Nugent et al. 1997; Höflich, Wheeler, & Thielemann 1998; Branch 1998) with high accretion rates, which permit relatively stable H- and He-shell burning and lead to a growing C/O white dwarf. When the white dwarf mass grows close to the Chandrasekhar mass, contraction sets in and the central density becomes high enough to ignite carbon fusion under degenerate conditions. The environment of a degenerate electron gas provides a pressure which depends only on the density. Therefore, the initial heat generation does not lead to pressure increase and expansion, which would result in controlled and stable burning. Instead, a thermonuclear runaway occurs. The burning front propagates through the whole star, causing complete disruption without a remnant.

The high Fermi energy of the degenerate electron gas in the white dwarf leads to efficient electron capture in the high density burning regions and reduces $Y_e = <Z/A>$, the electron fraction or equivalently the average proton to nucleon ratio, during explosive burning in the center. This is an important factor, controlling the isotopic composition ejected from such explosions (i.e., how neutron-rich is the matter produced). If the central density exceeds a critical value, electron capture can cause a dramatic reduction in the pressure of degenerate electrons and can therefore induce collapse (“accretion induced collapse”, AIC) of the white dwarf (Nomoto & Kondo 1991). Thus, electron capture on intermediate mass and Fe-group

nuclei plays a crucial role for the burning front propagation in SNe Ia. When Y_e 's are attained which correspond to the Z/A ratios of nuclei more neutron-rich than stability, the reverse beta-decays are also relevant.

Weak interactions describing electron/positron capture or beta-decay are either Fermi or Gamow-Teller transitions. Fermi transitions are only populating the isobaric analog state. Gamow-Teller transitions are distributed over many final states, with the maximum strength centered around the Gamow-Teller giant resonance. Folding these distributions with the thermal energy distribution of electrons (and the thermal population of target states) gives Gamow-Teller transitions the dominant role in burning at high temperatures and densities. Thus, in order to unravel the dynamics of the burning front propagation in SNe Ia, it is important to have an understanding of the Gamow-Teller strength functions in both the electron-capture and beta-decay reactions for unstable pf-shell nuclei. Up to present, astrophysical tabulations based on shell model matrix elements have been only available for nuclei in the sd-shell ($A=17-40$) (Fuller, Fowler, & Newman 1980). For heavier nuclei, more simplified approaches, based on average positions of the Gamow-Teller giant resonance and average matrix elements, were applied by the same authors for nuclei up to $A=60$, supplemented by existing experimental information (Fuller, Fowler, & Newman 1982, 1985, hereinafter denoted FFN). Revisions for sd-shell nuclei with accurate shell model wave functions and experimental transition strengths where available were calculated (Takahara et al. 1989; Oda et al. 1994), but for pf-shell nuclei the more appropriate shell model methods are only now becoming available. Aufderheide et al. (1994) performed a detailed study, in order to understand which nuclei are of primary importance for a variety of densities and Y_e values. They found $^{55-68}\text{Co}$, $^{56-69}\text{Ni}$, $^{53-62}\text{Fe}$, $^{53-63}\text{Mn}$, $^{64-74}\text{Cu}$, $^{49-54}\text{Sc}$, $^{50-58}\text{V}$, $^{52-59}\text{Cr}$, $^{49-54}\text{Ti}$, $^{74-80}\text{Ga}$, $^{77-80}\text{Ge}$, ^{83}Se , $^{80-83}\text{As}$, and ^{75}Zn to be important. These nuclei have recently been addressed with Quasi-particle Random Phase Approximation (QRPA) methods (Nabi & Klapdor-Kleingrothaus 1999), but more importantly, shell model diagonalization and shell model Monte Carlo approaches have also recently become available, which allow sufficiently accurate calculations in the pf-shell and at finite temperatures (Koonin, Dean, & Langanke 1997). First applications seem to reproduce the measured GT-distributions well and differ significantly from FFN (Dean et al. 1998; Caurier et al. 1999a,b).

The unfortunate situation is that until present there exist two sources of uncertainties in SNe Ia, related to either (i) the nuclear physics input discussed above or (ii) astrophysical modeling of the central ignition density ρ_{ign} and the flame propagation speed v_{def} in connection with hydrodynamic instabilities. Clear constraints for the latter can only be obtained when former is known with high accuracy. Though the white dwarf models can successfully account for the basic observational features of SNe Ia, the exact binary evolution that leads to SNe Ia has not yet been identified (see, however, Hachisu, Kato, & Nomoto 1999; Hachisu

et al. 1999). High accretion rates onto the white dwarf progenitor cause a stronger heating and thus a higher central temperature and pressure, which favor earlier ignition at lower densities ρ_{ign} . Carbon fusion apparently starts with a deflagration, i.e. a subsonic burning front (Nomoto, Thielemann, & Yokoi 1984). The propagation of the burning front occurs initially via heat conduction in the degenerate electron gas (with a burning front thickness of the order 10^{-4} - 10^{-5} cm). Instabilities of various scales lead to burning front propagation via convection and can accelerate the effective burning front speed. Multi-dimensional hydrodynamical simulations of the flame propagation have been attempted by several groups, though the results are still preliminary (Livne 1993; Arnett & Livne 1994; Khokhlov 1995; Niemeyer & Hillebrandt 1995; Niemeyer & Woosley 1997; Hillebrandt & Niemeyer 1997). These simulations have suggested that a carbon deflagration wave might initially propagate at a speed v_{def} as slow as a few percent of the sound speed v_s in the central region of the white dwarf. For example, Niemeyer & Hillebrandt (1995) obtained $v_{def}/v_s \sim 0.015$. After an initial deflagration in the central layers, the deflagration can turn into a detonation at lower densities ρ_{tr} (Khokhlov 1991; Woosley & Weaver 1994; Niemeyer 1999).

When summarizing the preceding discussion, we not notice that present modeling uncertainties in type Ia supernovae are related to ignition densities ρ_{ign} (progenitor evolution), the treatment of the burning front propagation with hydrodynamic instabilities (v_{def} and ρ_{tr}), and nuclear uncertainties for the electron capture rates on Fe-group nuclei in this high density and temperature environment. At temperatures exceeding 5×10^9 K, nuclear reactions involving strong plus electromagnetic forces are fast enough to attain a chemical equilibrium (in this context also referred to as Nuclear Statistical Equilibrium, NSE) which determines nuclear abundances on timescales much shorter than the typical burning front propagation times of the order of seconds. This reduces abundance uncertainties from the knowledge of reaction cross sections to those of masses and partition functions (Clayton 1983). But weak interactions act on longer timescales and their uncertainties enter directly. SNe Ia are the main producers of Fe-peak elements in the Galaxy (see e.g. the discussion in Iwamoto et al. 1999). Electron capture on nuclei in the incinerated material is responsible for the total neutron to proton ratio of matter and thus are crucial to the isotopic composition of Fe-group nuclei. The amount of electron capture depends on both v_{def} and ρ_{ign} . The central density of the white dwarf during ignition ρ_{ign} affects the electron chemical potential. The burning front speed v_{def} affects the time duration of matter at high temperatures, and with it the availability of free protons which can experience electron capture and the shape of the high energy tail of the electron energy distributions. Thus, the existing constraints for the production of neutron-rich Fe-group nuclei in SNe Ia can be translated into constraints for these parameters describing the burning front propagation.

In a recent paper we (Iwamoto et al. 1999) have attempted to find such constraints for

ρ_{ign} , v_{def} and ρ_{tr} via comparison with the solar Fe-group composition and chemical evolution models, but were still using the FFN electron capture rates. In the present paper we will test how dependent the conclusions are on variations and improvements to the set of weak interactions employed.

2. Weak Interactions in the Fe-Group

The systematic study of stellar weak interaction rates in the mass range of concern here ($A = 45 - 60$) was pioneered by Fuller, Fowler and Newman in a series of papers in the early eighties (Fuller, Fowler, & Newman 1980, 1982, 1985). These authors noticed the extraordinary role played by the Gamow-Teller (GT) giant resonance for stellar electron capture and, more strikingly, also for beta-decay. Unlike in the laboratory, β -decay under stellar conditions is significantly increased due to thermal population of the GT back resonances in the parent nucleus; the GT back resonances are the states reached by the strong GT transitions in the inverse process (electron capture) built on the ground and excited states (Fuller, Fowler, & Newman 1980, 1982, 1985), allowing for a transition with a large nuclear matrix element and increased phase space. Indeed, Fuller, Fowler and Newman concluded that the β -decay rates under collapse conditions are dominated by the decay of the back resonance. The relevant momentum transfers in type Ia supernovae is low enough to safely neglect the contributions of forbidden transitions to the weak interaction rates. Furthermore, the Y_e values encountered in type Ia supernovae stay large enough to involve only nuclei in NSE for which the GT transition is not Pauli-blocked; the latter is expected to happen for nuclei at the neutron shell closure $N = 40$ (Fuller 1982).

The GT contribution to the electron capture and β -decay rates has been parametrized by FFN on the basis of the independent particle model. To complete the FFN rate estimate, the GT contributions were supplemented by a contribution simulating low-lying transitions, using experimental data wherever possible. The FFN rates were updated and extended to heavier nuclei by Aufderheide et al. (1994). In recent years, however, the parametrization of the GT contribution, as adopted in FFN, became questionable when comparisons were made to upcoming experimental information about the GT distribution in pf-shell nuclei. These data clearly indicate that the GT strength is both quenched and fragmented over several states at modest excitation energies in the daughter nucleus (Alford et al. 1990, 1993; Vetterli et al. 1989; El-Kateb et al. 1994; Williams et al. 1995). Thus the need for an improved theoretical description was soon realized (Aufderheide 1991; Aufderheide et al. 1993; Aufderheide, Bloom, & Mathews 1993). It also became apparent that a reliable reproduction of the GT distribution in nuclei requires large shell model calculations which

account for all correlations among the valence nucleons in a major oscillator shell.

Such calculations in a complete major shell (usually referred to as $0\hbar\omega$ shell model calculations) are now possible using the recently developed Shell Model Monte Carlo (SMMC) (Johnson et al. 1992; Lang et al. 1993; Alhassid et al. 1994; Dean et al. 1994). Rather than solving the many-body problem by diagonalization of the Hamiltonian H , the SMMC method describes the nucleus by a canonical ensemble at temperature $T = \beta^{-1}$ and employs a Hubbard-Stratonovich linearization (Hubbard 1959; Stratonovich 1957) of the imaginary-time many-body propagator, $e^{-\beta H}$, to express observables as path integrals of one-body propagators in fluctuating auxiliary fields (Lang et al. 1993). Since Monte Carlo techniques avoid an explicit enumeration of the many-body states, they can be used in model spaces far larger than those accessible to conventional methods. The Monte Carlo results are in principle exact and in practice are subject only to controllable sampling and discretization errors. A comprehensive review of the SMMC method, a detailed description of the underlying ideas, its formulation, and numerical realization can be found in Koonin, Dean, & Langanke (1997).

Langanke et al. (1995) reported on the first complete pf -shell calculation of nuclei in the mass range $A = 50 - 62$. Most important for the present context, it reproduced all experimentally available total Gamow-Teller strengths GT_+ well, that is after scaling the spin operator with the universal quenching factor which accounts for the contribution of intruder states from outside the model space and appears to be A -independent within the pf -shell. [The GT_+ transitions describe the direction where a proton is changed into a neutron, like in electron capture or β^+ -decay.] However, stellar weak interaction rates have a strong phase space dependence and hence are more sensitive to the GT strength distribution in nuclei than to the total strength. The calculation of strength distributions within the SMMC method is in principle possible, but it involves a numerical inverse Laplace transform which is notoriously difficult to perform. Nevertheless Radha et al. (1997) succeeded in extracting SMMC GT_+ strength distributions for nuclei in the mass range $A = 50 - 64$ and again the agreement with data has been quite satisfactory. However, it became already apparent in Radha et al. (1997) that the SMMC model yields only an “averaged” GT strength distribution, as the statistical noise inherent in the Monte Carlo data allows only to determine the first moments of the distribution. Thus, the total strength, centroid and width are well reproduced via the inverse Laplace transform, but weak transitions to individual states outside the GT centroid distribution could not be resolved.

Motivated by the successful reproduction of all experimental GT_+ strength distributions, the SMMC approach has subsequently been used to calculate stellar electron capture rates for several nuclei in the mass range $A = 50 - 64$ (Dean et al. 1998). That study included

those nine nuclei for which experimental data are available ($^{54,56}\text{Fe}$, $^{58,60,62,64}\text{Ni}$, ^{51}V , ^{55}Mn , ^{59}Co), but it also predicted rates for other nuclei of interest for supernovae (^{45}Sc , $^{55,57}\text{Co}$, ^{56}Ni , $^{50,52}\text{Cr}$, $^{55,58}\text{Fe}$, and ^{50}Ti). We note that these calculations were the first which considered the complete $0\hbar\omega$ model space, and they also were consistently performed at finite temperature. The latter issue had been circumvented in earlier studies which assumed that the GT strength distributions on excited states are identical to the one built on the ground state, only shifted upwards in energy by the excitation energy of the parent state (FFN, Aufderheide et al. 1994).

When compared to the FFN parametrization of the GT centroids, the SMMC calculations showed some systematic deviations. Firstly, for even-even parent nuclei the GT_+ strength generally peaks at lower excitation energies in the daughter than was assumed by FFN. As a consequence one would intuitively expect the SMMC rates to be larger than the FFN rates for electron capture on even-even nuclei. However, they turned out to be approximately the same, since FFN often intuitively compensated for the smaller GT contribution (due to the shift in centroid) by an added low-lying transition strength. Secondly, for odd- A nuclei FFN have placed the GT centroid at significantly lower energies than found in the SMMC results and in the data. Consequently for these nuclei the GT contribution to the electron capture rate has been noticeably overestimated in FFN. Moreover for many odd- A nuclei the GT resonance part in the FFN parametrization dominates the capture rates, with the added low-lying strength component being rather unimportant. The SMMC calculations, on the other hand, indicate that the GT contribution to the rate should be reduced by nearly two orders of magnitude, making the rate sensitive to the weak transitions at low excitation energies in the daughter nucleus. This is a rather non-trivial situation for the SMMC approach, since these weak components in the GT distribution at low excitation energies are difficult to resolve, as mentioned above.

As the SMMC calculations suggest significant modifications of the stellar electron capture rates, we are motivated to investigate potential effects of these modifications on the dynamics and the nucleosynthesis. Unfortunately the SMMC rates available are not complete (Dean et al. 1998), as beta-decay rates are missing and the capture rates on odd- A nuclei should be supplemented by the contributions to low-lying states. These shortcomings can be overcome in large-scale shell model diagonalization calculations. These approaches have recently made significant progress and, combined with improved computer technologies, currently allow for diagonalization in model spaces large enough (involving typically 10 million or more configurations) to guarantee that the GT strength distribution is reasonably converged (Caurier et al. 1999a). Nevertheless shell model diagonalization is still a computationally formidable task and a complete compilation of weak stellar interaction rates, although possible, is a rather time-consuming project.

Recently stellar electron and beta-decay rates have been calculated by shell model diagonalization for several key nuclei (Martinez-Pinedo, Langanke, & Dean 1999; Langanke & Martinez-Pinedo 1998, 1999) and confirm the trend already observed in the SMMC studies. Systematic deviations from the GT parametrization assumed in the FFN compilation lead to significantly smaller electron capture rates on odd- A nuclei and odd-odd nuclei (even if the weak low-energy components are properly included). The diagonalization calculations yield, on average, slightly smaller capture rates on even-even nuclei than the FFN and the SMMC approaches. The latter is due to the fact that the diagonalization studies employed a slightly improved version of the residual interaction used in Dean et al. (1998). This correction removed the slight overestimation in the shell gap at the nucleon number $N = 28$, discussed in Langanke et al. (1995). The modified interaction reproduces quite nicely the ground state and prolate deformed bands in ^{56}Ni (Rudolph et al. 1999).

What consequences do the misplacement of the GT centroids have for the competing β decays? In odd- A and even-even nuclei (the daughters of electron capture on odd-odd nuclei) experimental data and shell model studies place the back-resonance at higher excitation energies than assumed by FFN. Correspondingly, its population becomes less likely at temperatures prevailing in a SN Ia. Hence the contribution of the back-resonance to the β decay rates for even-even and odd- A nuclei decreases. In contrast, the shell model β decay rate for odd-odd nuclei often are slightly larger than the FFN rates, because for these nuclei all available data, and all shell model calculations indicate that the back-resonance resides actually at lower excitation energies than previously parametrized.

To incorporate the modifications of the FFN rates, as suggested by the large shell model diagonalization studies, we follow the approximate procedure suggested in Martinez-Pinedo, Langanke, & Dean (1999). These authors compared the FFN and shell model rates for several typical nuclei and, based on this comparison, suggested to multiply the FFN electron capture rates by 0.2 (for even-even nuclei), 0.1 (odd- A), and 0.04 (odd-odd), while the FFN beta-decay rates might be scaled by 0.05 (even-even), 0.025 (odd- A) and 1.7 (odd-odd). In the following we will use these simple scalings to simulate potential modifications of the rates not provided by the SMMC approach. We emphasize here, however, that these scalings (denoted in the further discussion SMFA) are rather crude, and in principle are different for each nucleus and depend on temperature and density.

In Figures 1 and 2 the different versions of electron capture rates are plotted as a function of temperature for each nucleus for which SMMC electron capture rates are available. As the rates are a function of temperature and density, this includes implicitly the temporal evolution of the density up to the maximum temperatures attained, taken from the trajectory $(T(t), \rho(t))$ of the innermost zone of the SN Ia model WS15 discussed in the following section.

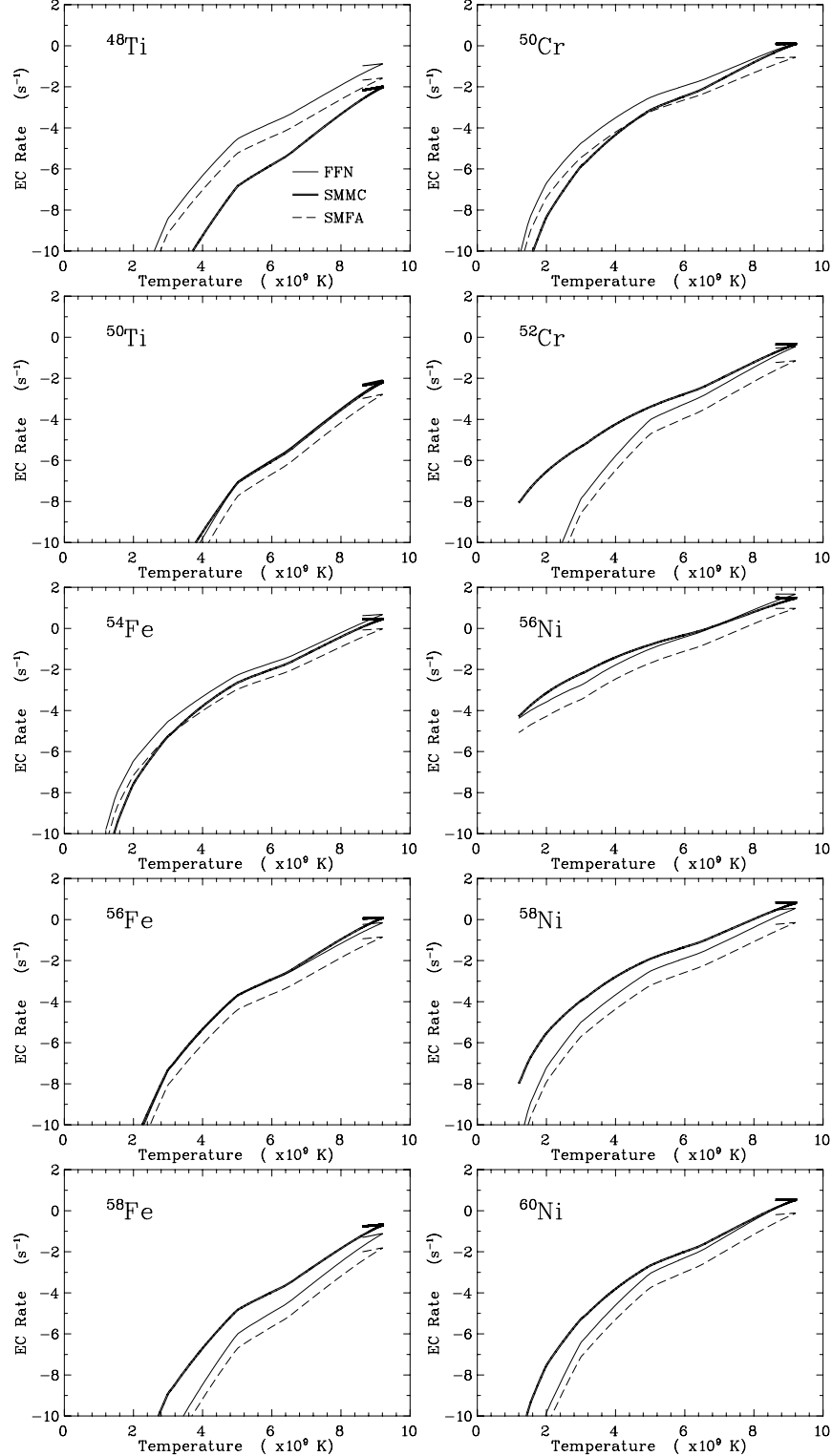


Fig. 1.— Electron capture rates [in s^{-1}] for even-even nuclei from different sources (FFN = Fuller et al.; Shell Model Monte Carlo SMMC = Dean et al. 1998; SMFA = estimates based on large-scale shell model diagonalization studies by Martinez et al. 1999). The rates are displayed as a function of temperature only, but reflect the temporal variation of density and temperature $\rho(t)$ and $T(t)$ in the trajectory of the innermost zone of model WS15.

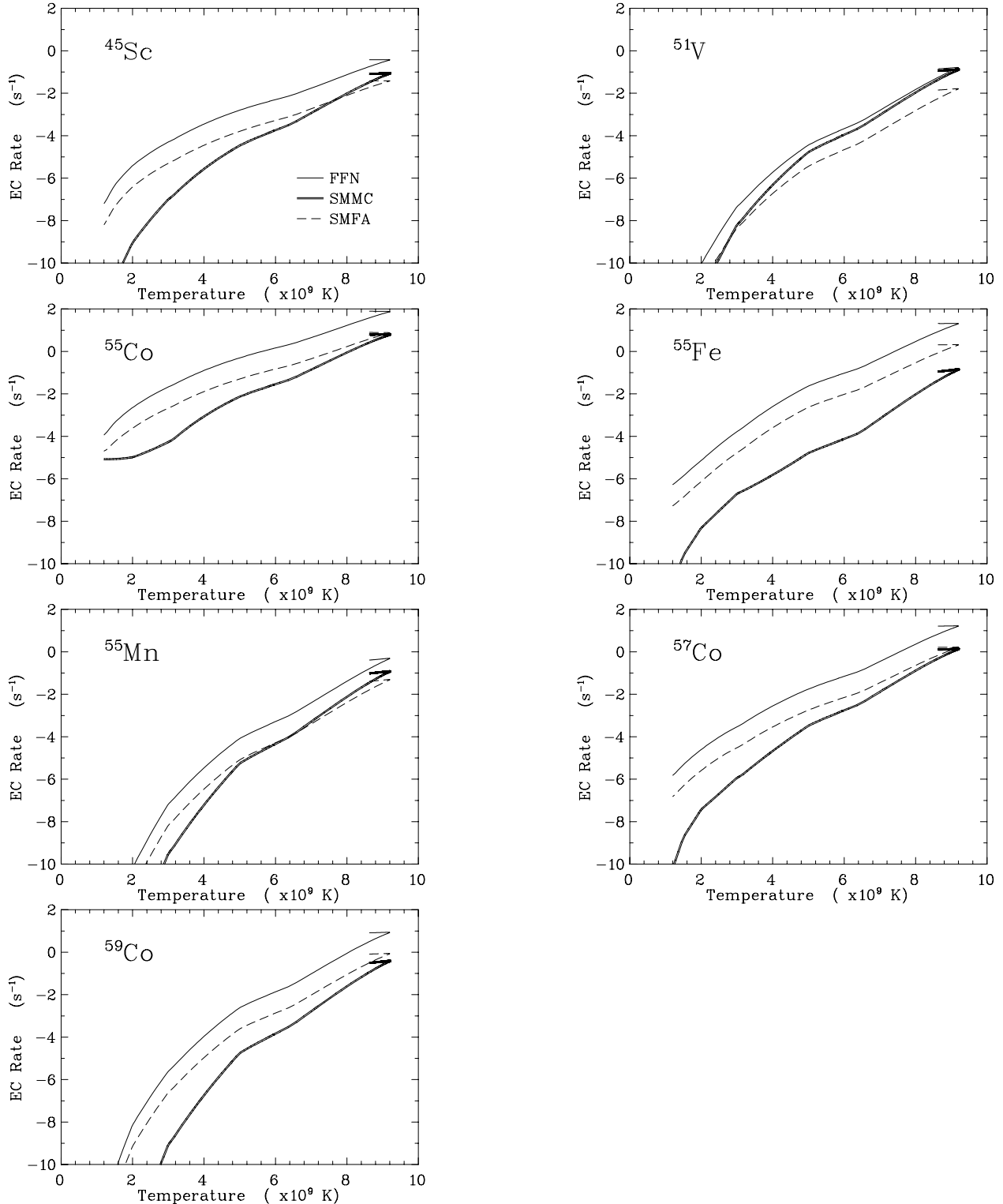


Fig. 2.— Same as Figure 1 for odd- A nuclei.

For the SMMC rates the systematic deviation from FFN are seen as mentioned earlier. For the even-even parent nuclei (Figure 1) both rates are approximately the same, at least when approaching higher temperatures. For the odd-A nuclei (Figure 2) SMMC rates are definitely smaller. The SMFA electron capture rates are also smaller than the FFN rates for both kinds of parent nuclei. When comparing SMMC and SMFA we see, that for odd-A nuclei the SMFA electron capture rates usually range (with the exception of ^{51}V) between FFN and SMMC. The fact that the SMFA rates are larger than the SMMC rates shows the importance of the low-lying transitions unresolved in SMMC approach as discussed above. For the even-even nuclei the SMFA rates are on average smaller than the SMMC rates. One reason for this change is the improved version of the residual interaction employed in Martinez-Pinedo, Langanke, & Dean (1999) in comparison to Dean et al. (1998), as discussed above. We do not show a comparison for odd-odd nuclei, because these rates are not available from the SMMC studies. But we refer to the discussion in the previous paragraph that there one expects the largest deviations.

3. SNe Ia Explosion Calculations

As shown in Thielemann, Nomoto, & Yokoi (1986) and reanalyzed in great detail in our recent paper (Iwamoto et al. 1999), electron capture is active on free protons and Fe-group nuclei during the early burning stage of a thermonuclear SN Ia explosion, when the burning front passes through the central region. Thus, electron capture neutronizes matter and reduces Y_e from its original value close to 0.5 (0.4989 if the abundances of nuclei other than ^{12}C and ^{16}O are due to a solar metallicity). This leads to the production of nuclei in the range between $N=Z$ and stability ($N>Z$). Only in exceptional cases also nuclei are produced which are more neutron-rich than stable species. This is also the reason why, opposite to conditions in core collapse supernovae (Martinez-Pinedo, Langanke, & Dean 1999), β^- decay does not play a prominent role. Thus, the most neutron-rich nuclei encountered already before β^+ -decay of unstable isotopes include species such as ^{48}Ca , ^{50}Ti , ^{54}Cr , and ^{58}Fe . Less neutron-rich (but also stable) nuclei like ^{54}Fe and ^{58}Ni are produced for more moderate Y_e values in the central zones of the SN Ia models. In Iwamoto et al. (1999) we made use of the FFN electron capture rates to predict the nucleosynthesis yields of Chandrasekhar mass models of SNe Ia. Those models employed variations in ρ_{ign} , v_{def} , and ρ_{tr} . As the outer (lower density) layers, where the deflagration-detonation transition can occur, are not affected by electron capture, we can neglect the third parameter ρ_{tr} in the present discussion. Here we show how the new electron capture rates affect the nucleosynthesis yields of the models WS15 and CS15. Those two models have the same burning front velocity, S15 denoting a slow deflagration of 1.5% of the local sound velocity, and differ in the ignition density at

thermonuclear runaway, $1.7 \times 10^9 \text{ gcm}^{-3}$ (C) and $2.1 \times 10^9 \text{ gcm}^{-3}$ (W).

Thielemann, Nomoto, & Yokoi (1986) showed that electron capture on free protons (which are not affected by uncertainties of pf-shell nuclei) dominates for the thermodynamic conditions in explosive burning zones of SNe Ia. In the case of the FFN rates they amount to about 60%. Thus, if electron capture rates of Fe-group nuclei are reduced by a factor of 10, this affects only the remaining 40%, and the full effect of a change in electron capture rates is a reduction from 100% to 64%. The difference in Y_e between the initial (almost symmetric) value of 0.4989 and the final value after explosive burning and electron captures is therefore reduced with respect to the FFN calculations by about a factor 0.64. This point is the key to understanding results from calculations with different sets of electron capture rates.

In our previous studies we noted that the ignition density is a quantity which greatly influences the amount of electron capture in the central layers. The higher ignition density of WS15 increases the Fermi energy and therefore the electron capture rates, which leads to a smaller Y_e when compared to CS15. Therefore, WS15 synthesizes more neutron-rich nuclei than CS15. With the FFN rates used in Iwamoto et al. (1999) this led to a strong overproduction of ^{50}Ti and ^{54}Cr in comparison to the corresponding solar values for WS15. Consequently model CS15 seemed to be preferable in avoiding overabundances of the neutron-rich nuclei. While ρ_{ign} shifts the average Y_e -value of the central layers, the burning front speed v_{def} determines the gradient of $Y_e(r)$. Information passes with sound speed to the outer layers. Here a small v_{def} permits a longer time for expansion to lower densities before the arrival of the burning front. This reduces the effect of electron capture in the outer layers of the central core and steepens the Y_e gradient. Thus, while ρ_{ign} is mostly responsible for the minimum Y_e -values which are attained in the central layers, v_{def} controls the amount of matter with intermediate Y_e -values (like e.g. ^{54}Fe and ^{58}Ni) by determining the Y_e -gradient. We will analyze here how variations in electron capture rates influence the conclusions drawn earlier for ρ_{ign} and v_{def} .

The rates employed in our calculations were as follows: (i) FFN rates as a benchmark for the further comparison (these rates were taken from Fuller, Fowler, & Newman (1982a) and hence do not incorporate any quenching of the GT strength); (ii) inclusion of the electron captures rates calculated within the SMMC method by replacing the corresponding FFN rates. SMMC rates were used for the parent nuclei ^{45}Sc , $^{48,50}\text{Ti}$, ^{51}V , $^{50,52}\text{Cr}$, ^{55}Mn , $^{54-56,58}\text{Fe}$, and $^{55,57,59}\text{Co}$, $^{56,58,60}\text{Ni}$. For nuclei not mentioned above (where no SMMC calculations were available), the rates were taken from FFN; (iii) to simulate potential modification of the rates not provided by the SMMC method, we also multiplied the FFN electron capture and beta-decay rates within the Fe-group nuclei by these factors, derived from comparison between

FFN and shell model rates (see section 2). These modified SN Ia models are labeled with SMFA; (iv) A further option is to treat even-even (ee), odd-A (oa), and odd-odd (oo) nuclei in different ways, in order to test the sensitivity of the models and the importance of certain rates in particular nuclei. Such calculations are denoted by SMFA with the corresponding extension ee, oa, oo or by combinations, e.g. ee+oa. With these modifications of the electron capture rates we recalculated the nucleosynthesis for the SN Ia models WS15 and CS15. Resulting deviations from the FFN models of Iwamoto et al. (1999) are discussed in the following two subsections.

3.1. Influence on Abundances and Y_e -Patterns

In general, the updated electron capture rates are smaller than the FFN rates. Thus the central region of the exploding white dwarf experiences less electron captures and the SN Ia nucleosynthesis yields should be less neutron-rich. Therefore, Y_e^{SMMC} and Y_e^{SMFA} should be larger than Y_e^{FFN} in the central layers and the overabundances of the neutron-rich nuclei ^{54}Cr and ^{50}Ti in WS15 should be reduced. The central Y_e -value, $Y_{e,c}$, of different models and different electron capture rate sets are listed in the Table 1. In the case of SMMC the final $Y_{e,c}$ value of the model WS15 increased from 0.440 (FFN) to 0.441. For the model CS15, which has a smaller ignition density leading to a higher $Y_{e,c}$ than WS15, the final $Y_{e,c}$ -value changed from 0.449 (FFN) to 0.451 (see Figure 3a and c). On average the Y_e^{SMMC} -values for the central layers are about 0.002 larger than Y_e^{FFN} for both models (Figure 3d).

Table 1: Neutron-rich Nucleosynthesis of specific nuclei with mass fraction X_i ; $X_i/X(^{56}\text{Fe})/(X_i/X(^{56}\text{Fe}))_{\odot}$

Model	$Y_{e,c}$	^{50}Ti	^{54}Cr	^{58}Fe	^{64}Ni	^{62}Ni	^{54}Fe	^{58}Ni
WS15 FFN	0.4396	5.3	9.8	2.6	1.1	2.5	1.2	2.7
WS15 SMMC	0.4411	3.8	7.7	2.1	0.7	2.4	1.2	2.7
WS15 SMFAee+oa	0.4424	2.9	6.4	1.8	0.5	2.3	1.2	2.6
WS15 SMFA	0.4507	0.6	2.3	1.0	0.01	2.0	1.2	2.6
CS15 FFN	0.4491	0.5	2.1	0.9	0.01	1.9	1.3	2.7
CS15 SMMC	0.4513	0.2	0.9	0.5	0.004	1.8	1.2	2.7
CS15 SMFA	0.4594	0.008	0.008	0.007	0.0002	1.6	1.2	2.6

Bearing in mind that SMMC electron capture rates are available for certain even-even and odd-A nuclei only, and that for the latter it is difficult to resolve the transitions at

low-lying excitations in the SMMC approach, it is important to test which type of nuclei are mostly responsible for the resulting Y_e -shift. One of the tests involves the application of SMMC rates only for even-even nuclei, while using FFN rates for all other nuclei. This is denoted by the label SMMCEE. It is evident from the Y_e -curve in Figure 3a that this case is almost identical with FFN, implying that the major cause for the difference between FFN and SMMC is due to capture on odd-A nuclei. This underlines that electron capture on even-even nuclei seems unimportant despite their large abundances in nuclear statistical equilibrium. The reason is that rates for even-even nuclei (with which these abundances have to be multiplied) are very small due to large energy thresholds.

In order to investigate the size of the Y_e -changes resulting from uncertainties between SMMC and the average factors (SMFA) deduced from large-scale shell model calculations, we replaced the 17 SMMC electron capture rates by the corresponding scaled FFN rates (labeled SMFATest). Figure 3a shows that both Y_e -curves are very similar. Therefore, it seems that the SMFA and SMMC odd-A rates yield comparable Y_e -results, indicating a similar behavior. This can be explained by the fact that most of the electron captures occur at high temperatures where the low-lying GT strength (which differs in both SMMC and SMFA approaches) is less important. As a result, for odd-A nuclei the use of SMFA factors or the Monte Carlo shell model (SMMC) leads to similar results. (The same holds true for even-even rates, as shown above).

When scaling *all* FFN rates that are used in the network as suggested by the shell model diagonalization calculations (label SMFA), i.e. not only those for which SMMC rates were available, we see in Figure 3b, c, and d that Y_e^{SMFA} is about 0.008 larger than Y_e^{FFN} for WS15 as well as CS15. The central Y_e -value increased from 0.440 to 0.451 (WS15) and from 0.449 to 0.459 (CS15), as listed in Table 1. The deviation from FFN is much larger than for SMMC. This could have two possible causes. (i) A more complete set of modified electron capture rates is used, 17 (SMMC) versus 79 (SMFA). (ii) Odd-odd parent nuclei are missing in the SMMC calculations and could be important. In order to test which aspect plays the more important role, we chose a subset where only even-even and odd-A nuclei were multiplied with the average SMFA factors (labeled SMFAee+oa in Figure 3b). Thus, this case ignores modifications for odd-odd nuclei, while the multiplication by SMFA factors for even-even and odd-A nuclei should differ little from the use of SMMC rates as shown in the previous paragraph. Therefore, the comparison of SMFAee+oa with SMMC measures the impact of the increased number of modified electron capture rates, and the comparison to SMFA shows the influence of odd-odd nuclei. The resulting Y_e -curve (Figure 3b) displays a small Y_e shift between SMMC and SMFAee+oa, and a larger Y_e -shift between SMFAee+oa and SMFA. Therefore, the inclusion of odd-odd nuclei has the largest influence on the Y_e difference between SMFA and SMMC.

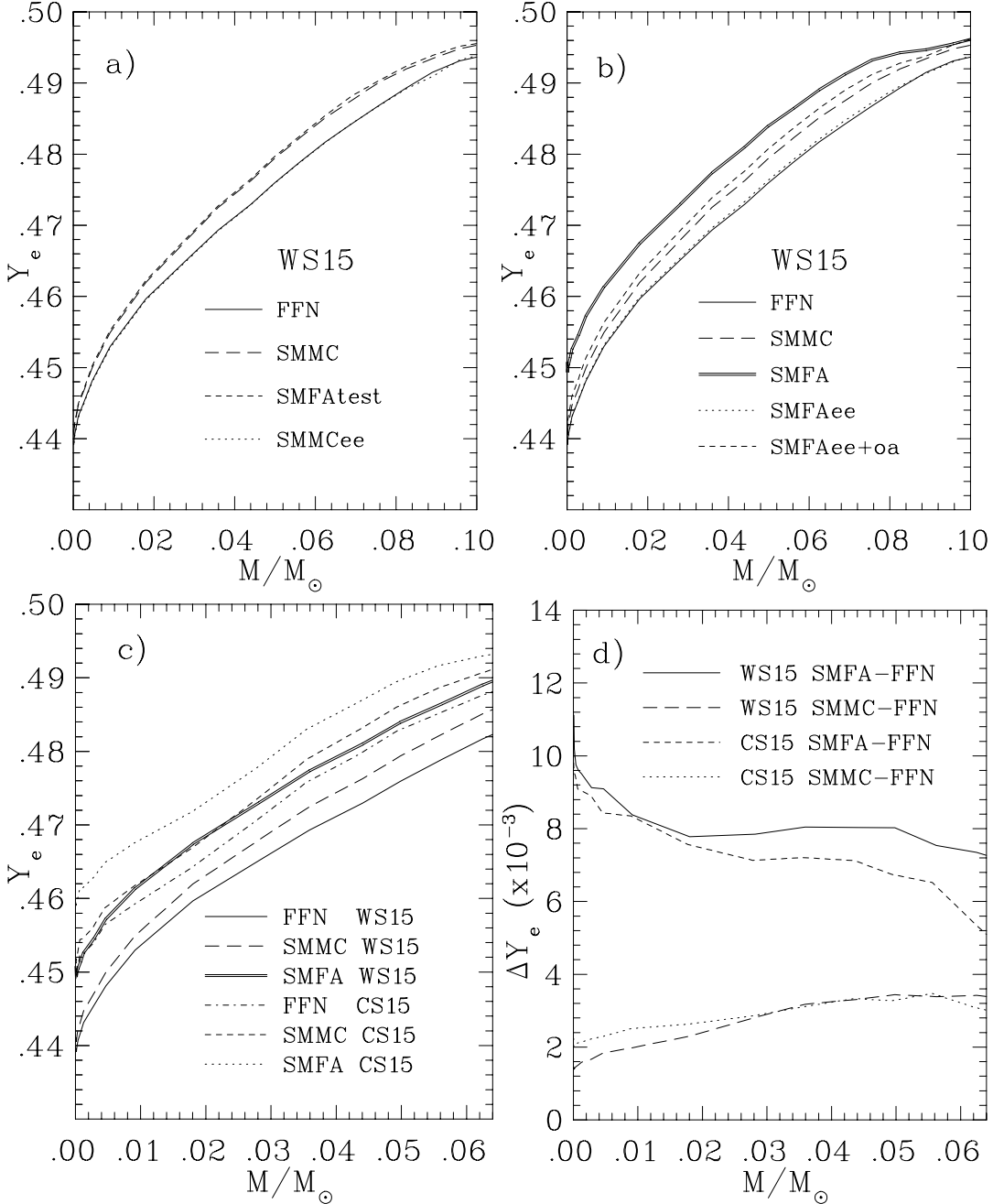


Fig. 3.— Y_e , the total proton to nucleon ratio and thus a measure of electron captures on free protons and nuclei, after freeze-out of nuclear reactions as a function of radial mass for different models and electron capture rates. Also the Y_e -difference ΔY_e between various cases is shown at the bottom right (d). A detailed discussion of the changes with different electron capture rate sets is given in the text. Notice, however, that the changes for a given model (here WS15 and CS15) lead to almost parallel Y_e -curves in the intermediate Y_e -range responsible for the major abundances of ^{54}Fe and ^{58}Ni . This can also be seen in the close to constant ΔY_e -curves in (d). Thus, a change in electron capture rates does (to first order) not affect the Y_e -gradient of a model.

Thus, we have shown that the rate change for odd-A nuclei is mostly responsible for the Y_e -shift between FFN and SMMC, and that the inclusion of odd-odd nuclei causes the largest part of the Y_e -shift between SMMC and SMFA. This makes clear that the changes in the electron capture rates for odd-A and odd-odd nuclei are responsible for the Y_e difference between SMFA and FFN, while the contribution of even-even nuclei is negligible, an assertion which was directly tested by case SMFAee (Figure 3b). As odd-odd nuclei are difficult to treat within the shell model Monte Carlo approach, a further improvement would be the direct use of large-scale shell model diagonalization calculations. In the present paper we provide preliminary results by applying average factors (SMFA) derived from detailed calculations of a few key nuclei (Martinez-Pinedo, Langanke, & Dean 1999)

To examine the impact of these changes in weak rates on individual species, we show in Figure 4 the radial distribution of a few key abundances for the three select cases FFN, SMMC, and SMFA. The abundance pattern is very similar, but each abundance curve is shifted inwards in the sequence FFN, SMMC, and SMFA. This makes clear that FFN reaches the smallest central Y_e 's, resulting in abundance peaks of ^{50}Ti , ^{54}Cr , and ^{58}Fe close to the center, while these peaks are cut off for SMFA. Neglecting this very central behavior, one can recognize, however, that the total amount of intermediate Y_e nuclei like $^{54,56}\text{Fe}$ and ^{58}Ni is essentially unaffected (see also Table 1). This is in accordance with the results of Figure 3, where we see that the Y_e -gradient is almost identical and the ΔY_e 's close to constant for models which apply different sets of electron capture rates. Note that only the onset of the Y_e -reduction due to electron captures is shifted as a function of $M(r)$. This leaves the same amount of mass composed of these intermediate Y_e nuclei. The main difference is in the central Y_e values attained and as a result in the amount of the most neutron-rich nuclei.

As the Y_e gradient is determined by v_{def} (see Iwamoto et al. 1999) and apparently is not changed by different sets of electron capture rates, we can conclude that the consequences for the permitted range of burning front speeds remain the same. In Iwamoto et al. (1999) we determined this range v_{def}/v_s to be of the order 0.015-0.03. The central neutronization is however dependent on ρ_{ign} and, as shown here, on the set of electron capture rates employed. Thus, we have to expect that our previous conclusions for the ρ_{ign} -range might have to be changed. We will discuss this further in the following subsection.

3.2. Comparison to Solar Abundances

The solar element abundances are a snapshot of the local galactic abundance distribution at the formation of the solar system 4.5×10^9 years ago. The heavy elements in the Galaxy originate from the ejected matter of supernovae, with SN Ia. SNe Ia being responsible for

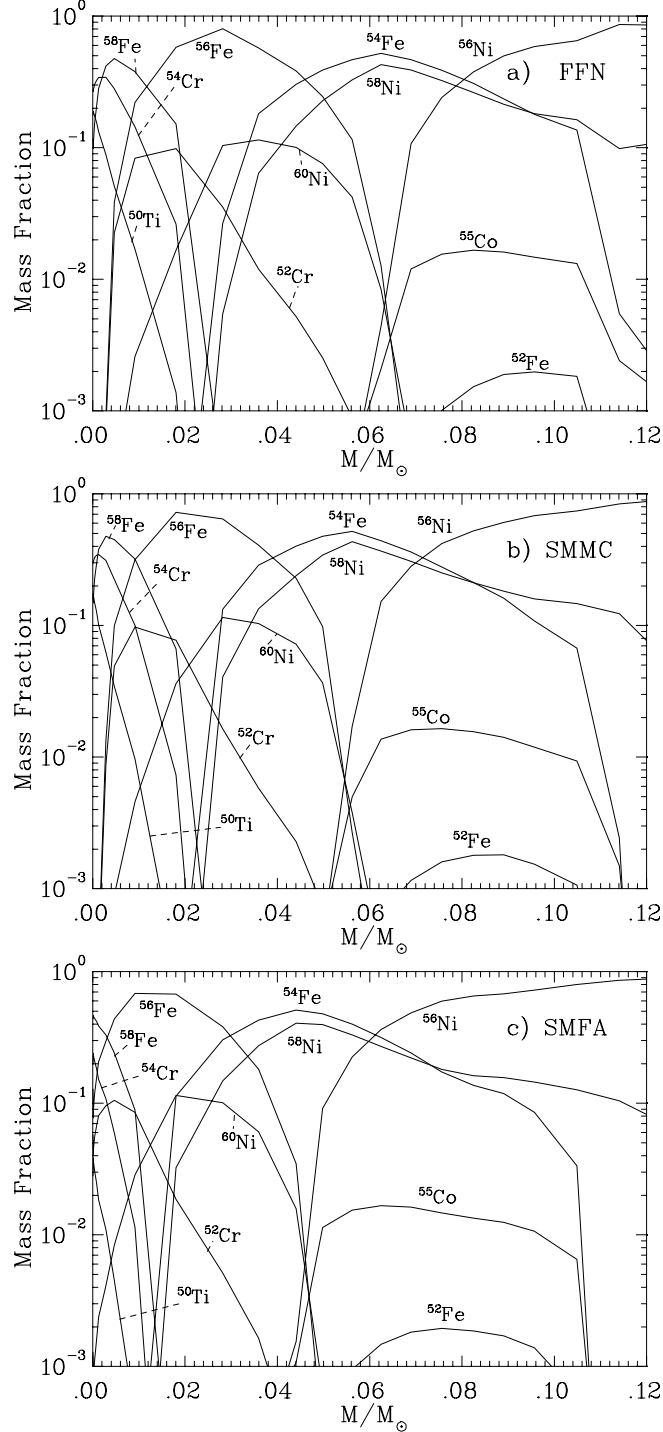


Fig. 4.— Central abundances in model WS15 for different electron capture rates: (a) FFN, (b) Shell Model Monte Carlo (SMMC), (c) FFN multiplied with average factor estimates from large-scale shell model diagonalization studies (SMFA).

55% or more of the Fe-group elements in the Galaxy (see the discussion in Iwamoto et al. 1999). Thus, the ejecta of SNe Ia can contain an overabundance in comparison with the solar values of no more than a factor of two among the Fe-group nuclei. This is the maximum for species which have no other production site than SNe Ia and would have to be reduced accordingly if alternative sources contribute as well. This provides constraints for the nucleosynthesis results of SNe Ia models. In Iwamoto et al. (1999), where we used the FFN electron capture rates only, we concluded that CS15 was a better model compared to WS15 in terms of avoiding overproduction of neutron-rich nuclei. This would indicate that for the majority of white dwarfs undergoing a thermonuclear runaway and SNe Ia events, the central density should be lower than $\sim 2 \times 10^9 \text{ g cm}^{-3}$, though the exact constraint depends somewhat on the flame speed.

Now, with the new sets of electron capture rates, the situation has changed. The new smaller rates reduce the production of neutron-rich nuclei. In Figures 5, 6, and 7 and in Table 1 the ratios to solar abundances (normalized to ^{56}Fe) are displayed for WS15 and CS15 employing different types of electron capture rates. Here the results of the central slow deflagration studies have been merged with (fast deflagration) W7 compositions for the outer layers (Nomoto et al. 1994; Thielemann, Nomoto, & Yokoi 1986; Thielemann et al. 1997; Iwamoto et al. 1999). In the outer layers the densities are sufficiently low that electron capture does not modify the pre-explosion value of Y_e . (Y_e in these layers is only a witness of the initial metallicity of the white dwarf, manifesting itself in the amount of ^{22}Ne , which resulted in H and He-burning from the initial CNO isotopes.) Thus, the same model results for these outer layers can be added for different sets of electron capture rates.

For SMMC the overabundances of the most neutron-rich nuclei in WS15 is reduced to 75% in comparison to the FFN calculations. ^{50}Ti and ^{54}Cr are still significantly overabundant though. ^{58}Fe is now reduced to about the limit of a factor 2. All three nuclei originate from the very center. The small overabundance of ^{58}Ni and ^{62}Ni remains (being due to the Y_e -gradient and thus v_{def} rather than ρ_{ign} and the choice of electron capture rates). In CS15 the abundance of ^{54}Cr is reduced strongly. Again, a slight overabundance of ^{58}Ni is noticed. Thus, the effect of the use of SMMC over FFN is the same in both models, while the difference between WS15 and CS15 remains that the former is more neutron-rich in the center, due to a higher ρ_{ign}). For SMFA the overabundance of the neutron-rich nuclei is reduced to about 20% of the results obtained with FFN. In model WS15 the nuclei ^{50}Ti , ^{58}Fe , and ^{62}Ni are now produced within a factor of 2 of solar values. Only a very slight overproduction of ^{54}Cr and ^{58}Ni remains, the latter being mostly dependent on the Y_e -gradient (due to v_{def}) and unaffected by the rate change.

^{50}Ti , ^{54}Cr , and ^{58}Fe , which are the dominant species in matter with a Y_e -value below

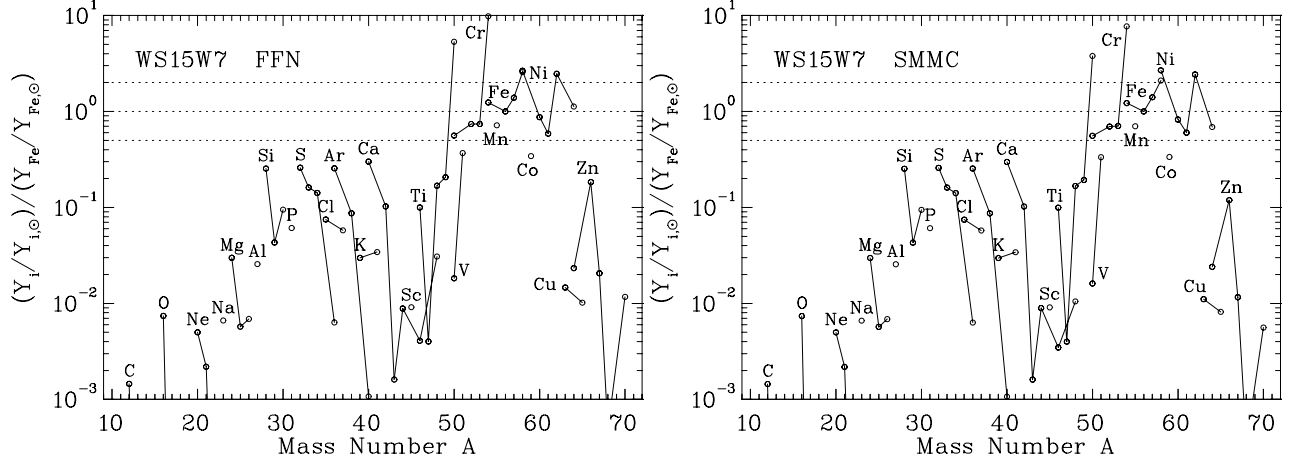


Fig. 5.— Ratio of abundances to solar predicted in model WS15 for different electron capture rate sets. Isotopes of one element are connected by lines. The ordinate is normalized to ^{56}Fe . Intermediate mass elements exist, but are underproduced by a factor of 2-3 for SNe Ia models in comparison to Fe-group elements. The Fe-group does not show a composition close to solar. Especially ^{54}Cr and ^{54}Fe are strongly overproduced by more than a factor of 3. The change from FFN rates (top) to SMMC (bottom) reduces the overproduction over solar to about 75%.

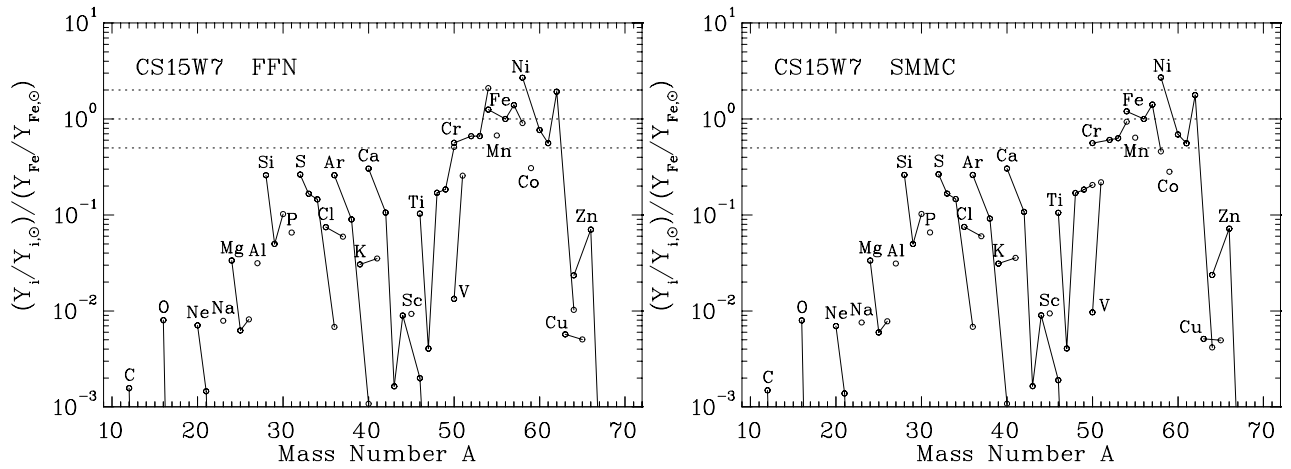


Fig. 6.— Similar to Figure 5 but for model CS15. The slight overproduction of ^{54}Cr is reduced to solar ratios while ^{50}Ti is even underproduced by more than a factor of 3.

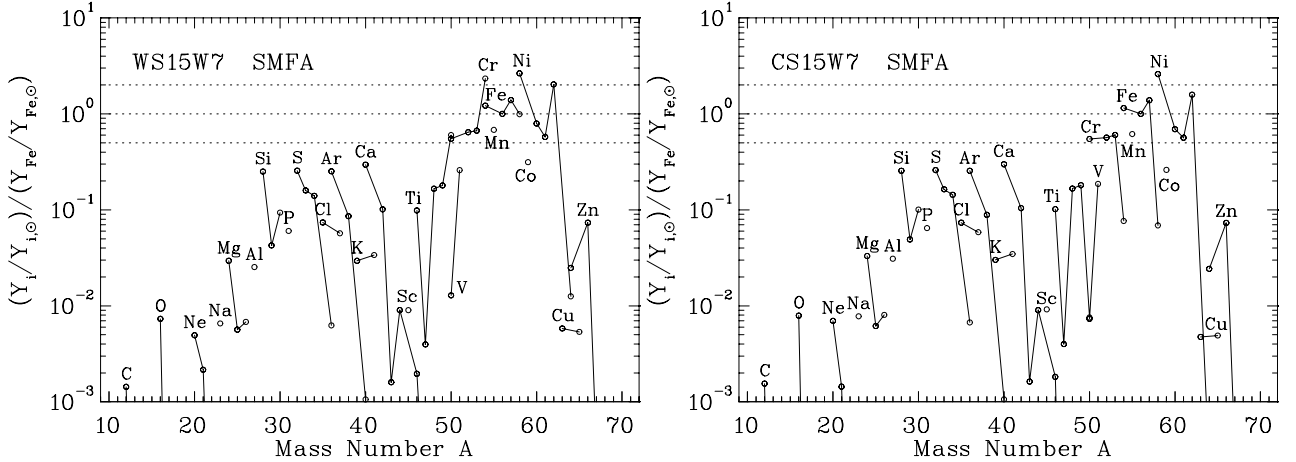


Fig. 7.— Similar to Figure 5 but for models WS15 and CS15, in both cases with estimates of average factors (SMFA) from large-scale shell model calculations for all nuclei. Even for WS15 the overproduction is reduced close to the acceptable limit of a factor of 2. ^{50}Ti and ^{54}Cr are now underproduced in CS15.

0.452, are strongly reduced in WS15 for the rate set SMFA, because the central $Y_{e,c}$ of 0.451 is larger than 0.440 found using FFN. The number of mass zones with Y_e below 0.452 is therefore much smaller. This radial shift and central cut-off of the Y_e -curve and its result on abundances have already been discussed in relation to Figure 4 in section 3.1. The nuclei ^{58}Ni and ^{54}Fe are the dominant products for Y_e between 0.470 and 0.485, which extends over a very similar range of integrated masses for all rate sets. The same is true for ^{56}Fe , which is produced for Y_e values between 0.46 and 0.47. The total ^{62}Ni abundance stems partially from ^{62}Ni synthesized in the very center but is also partly due to the decay of ^{62}Zn in the alpha-rich freeze-out zones of the outer core layers whose Y_e is dominated by metallicity rather than electron capture (Thielemann, Nomoto, & Yokoi 1986; Thielemann et al. 1997; Iwamoto et al. 1999). Therefore, the reduction of the abundance of this nucleus in the central sites does not affect the total value as much as is the case of ^{54}Cr and ^{50}Ti , which both originate from central regions.

In comparison to the previous calculations employing FFN rates, the model WS15 experiences strong improvement (i.e. reduction) in the overproduction of neutron-rich nuclei when applying the new sets of electron capture rates. Model CS15, which showed no significant overproduction for the neutron-rich nuclei with FFN rates, still exhibits this same behavior. In fact, the reduced electron capture rates cause a strong underproduction of neutron-rich nuclei like ^{50}Ti and ^{54}Cr in CS15. Thus, the modified electron capture rates change the outcome of SN Ia models. They certainly permit the higher ignition densities of model W ($2.1 \times 10^9 \text{ g cm}^{-3}$). If some of these neutron-rich nuclei originate only from SNe

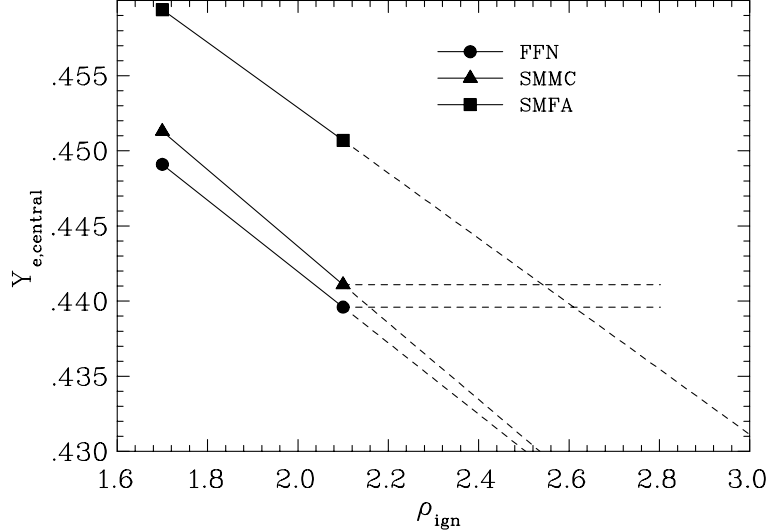


Fig. 8.— Change of central Y_e -values obtained for models CS15 and WS15 (with increasing ignition densities ρ_{ign} in units of 10^9 g cm^{-3}) for different electron capture rate sets FFN, SMMC, and SMFA. If this trend continues to higher ignition densities in a similar way as the rough extrapolation indicated by dashed lines, the use of SMFA would lead to the same Y_e -value as WS15 with FFN for an ignition density of $\rho_{ign} = 2.6 \times 10^9 \text{ g cm}^{-3}$. This corresponds to an increase of a factor of 1.24 in ρ_{ign} .

Ia, a shift for the average SN Ia close to this higher ρ_{ign} of model W might even be needed. We have not yet addressed a possible upper limit for ρ_{ign} when utilizing the present SMFA rate set. A rough estimate can be obtained from Figure 8, where we show the central Y_e as a function of ρ_{ign} obtained with different electron capture rate sets, making use of models CS15 ($\rho_{ign} = 1.7 \times 10^9 \text{ g cm}^{-3}$) and WS15 ($\rho_{ign} = 2.1 \times 10^9 \text{ g cm}^{-3}$). If the trend continues in a similar way as experienced between models C and W, we would expect a central Y_e -value comparable to that of WS15 with FFN rates for $\rho_{ign} = 2.6 \times 10^9 \text{ g cm}^{-3}$ when utilizing SMFA. This corresponds to an increased ignition density by about a factor of 1.24 when shifting from FFN to SMFA rates.

4. Summary

The need for an improved theoretical description of electron capture rates for pf-shell nuclei beyond the early phenomenological tabulations by Fuller, Fowler, & Newman (1980, 1982, 1985) was realized by Aufderheide (1991) and Aufderheide et al. (1993); Aufderheide,

Bloom, & Mathews (1993), calling for large shell model calculations which account for all correlations among the valence nucleons in a major oscillator shell. Motivated by the successful reproduction of all experimental GT_+ strength distributions, the Shell Model Monte Carlo approach (SMMC) was recently applied to calculate stellar electron capture rates for several nuclei in the mass range $A = 50 - 64$ (Dean et al. 1998). The resulting significant modifications of stellar electron capture rates motivated the present investigation into potential effects on the dynamics and the nucleosynthesis of SNe Ia.

The SMMC approach has, however, some limitations and requires supplemental input. It makes use of a continuous strength distribution while the capture rates on odd- A nuclei should be supplemented by the contributions to low-lying states. In addition, rates for odd-odd nuclei are currently not available. Thus, although SMMC calculations are generally substantiated by large-scale shell model diagonalization calculations, information concerning this low lying GT strength requires presently the use of the latter approach. These approaches have recently made significant progress (Caurier et al. 1999a). For a preliminary and approximate treatment we followed the procedure outlined by Martinez-Pinedo, Langanke, & Dean (1999), who suggested to multiply the FFN electron capture rates with averaged factors for even-even, odd- A , and odd-odd nuclei.

These electron capture rate modifications affect the early burning stage of a thermonuclear SN Ia explosion, being mostly responsible for the formation of neutron-rich nuclei such as ^{48}Ca , ^{50}Ti , ^{54}Cr , $^{54,58}\text{Fe}$, and ^{58}Ni in the innermost zones of the SN Ia models. Our nucleosynthesis calculations show that, when the rates are multiplied with nuclear abundances, the odd-odd and odd- A nuclei cause the largest contribution to the neutronization of nucleosynthesis ejecta and are essentially responsible for the Y_e -change, while the contribution of even-even nuclei is negligible. The present investigation focuses on the question whether our earlier conclusions drawn for model parameters like central ignition density ρ_{ign} , speed of the (deflagration) burning front v_{def} , and the transition density from deflagrations to detonations ρ_{tr} (Iwamoto et al. 1999), based on FFN electron capture rates, would be affected.

The transition density is always of the order 10^7 g cm^{-3} , where electron capture rates are too slow on the dynamical timescales involved. Thus, earlier conclusions drawn for this parameter are unaffected. We found in the present analysis that the Y_e -gradient is only determined by v_{def} and apparently does not change with the set of electron capture rates. Therefore, the conclusions for the permitted range of burning front velocities also remain the same. In Iwamoto et al. (1999) we determined this range v_{def}/v_s to be of the order 0.015-0.03.

The central neutronization, however, is dependent on ρ_{ign} and - as shown here - on the rate set of electron captures employed. Thus the modified electron capture rates change the

outcome of SN Ia yields. In comparison to the previous calculations with FFN rates, the model W ($\rho_{ign}=2.1 \times 10^9 \text{ g cm}^{-3}$) experienced a strong reduction in the overproduction of neutron-rich nuclei when applying the new sets of electron capture rates. In fact, they lie within the permitted uncertainties of solar Fe-group abundances. Model C ($\rho_{ign}=1.7 \times 10^9 \text{ g cm}^{-3}$), which showed no significant overproduction for the neutron-rich nuclei with FFN rates, still exhibits the same behavior. In fact, the reduced electron captures rates cause a strong underproduction of neutron-rich nuclei like ^{50}Ti and ^{54}Cr . The rate modifications thus permit higher ignitions densities than previously expected, by about a factor of 1.24. If some of these nuclei originate only from SNe Ia, the a shift to these higher ρ_{ign} might be needed for the average SN Ia.

This work should, however, be completed using a full set of shell model weak interaction rates. In addition, strong Coulomb coupling between ions and electrons lowers the electron capture Q-values and thus the threshold densities (Cough & Arnett 1973; Bravo & Garcia-Senz 1999). Such a behavior, which is similar to the screening of charged particle capture rates, has not yet been taken into account in nucleosynthesis studies, but its importance should be tested. Some of the conclusions drawn here could be reversed, as its effect would cause an enhancement of electron capture rates.

This work has been supported in part by the Swiss Nationalfonds (2000-53798.98), the US Department of Energy (DOE contracts DE-AC05-96OR22464 and DE-FG02-96ER40983), the Danish Research Council, the grant-in-Aid for COE research (07CE2002) of the Ministry of Education, Science, and Culture in Japan, a fellowship of the Japan Society for the Promotion of Science for Japanese Junior Scientists (6728), Some of us (KN and FKT) thank the Aspen Center for Physics for hospitality and inspiration during the 1999 Type Ia supernova program.

REFERENCES

Alford, W.P., et al. 1990, Nucl. Phys., A514, 49
Alford, W.P., et al. 1993, Phys. Rev., C48, 2818
Alhassid, Y., Dean, D.J., Lang, G.H., & Koonin, S.E. 1994, Phys. Rev. Lett., 72, 613
Arnett, W.D. & Livne, E. 1994, ApJ, 427, 314
Aufderheide, M.B. 1991, Nucl. Phys., A526, 161

Aufderheide, M.B., Bloom, S.D., Ressler, D.A., & Mathews, G.J. 1993, Phys. Rev., C47, 2961

Aufderheide, M.B., Bloom, S.D., & Mathews, G.J. 1993, Phys. Rev., C48, 1677

Aufderheide, M., Fushiki, I., Woosley, S.E., Hartmann, D. 1994, Ap. J. Suppl., 91, 389

Branch, D. 1998, Ann. Rev. Astron. Astrophys. 36, 17

Bravo, E., & Garcia-Senz, D. 1999, MNRAS 307, 984

Caurier, E., Langanke, K., Martinez-Pinedo, G., Nowacki, F. 1999, Nucl. Phys. A653, 439

Caurier, E., Martinez-Pinedo, G., Nowacki, F., Poves, A., Retamosa, J., Zuker, A.P. 1999, Phys. Rev. C59, 2033

Clayton, D.D. 1968, 1983, *Principles of Stellar Evolution and Nucleosynthesis*, Univ. of Chicago Press

Couch, R.G., & Arnett, W.D. 1973, ApJ 180, L101

Dean, D.J., Koonin, S.E., Langanke, K., Radha, P.B., Alhassid, Y. 1995, Phys. Rev. Lett. 74, 2909

Dean, D.J. Langanke, K., Chatterjee, L., Radha, P.B., Strayer, M.R. 1998, Phys. Rev. C58, 536

El-Kateb, S., et al. 1994, Phys. Rev. C49, 3128

Fuller, G.M. 1982, Ap. J. 252, 741

Fuller, G.M., Fowler, W.A., Newman, M. 1980, Ap. J. Suppl. 42, 447

Fuller, G.M., Fowler, W.A., Newman, M. 1982, Ap. J. Suppl. 48, 279

Fuller, G.M., Fowler, W.A., Newman, M. 1982a, <http://ie.lbl.gov/astro/fuller.html>

Fuller, G.M., Fowler, W.A., Newman, M. 1985, Ap. J. 293, 1

Hachisu, I., Kato, M., & Nomoto, K. 1999a, ApJ, 522, L43

Hachisu, I., Kato, M., Nomoto, K., & Umeda, H. 1999b, ApJ, 519a, 314

Hillebrandt, W., Niemeyer, J.C. 1997, in *Thermonuclear Supernovae*, eds. P. Ruiz-Lapuente, R. Canal, J. Isern, Kluwer Academic, p.337

Höflich, P., & Khokhlov, A. 1996, ApJ, 457, 500

Höflich, P., Khokhlov, A. Wheeler, J.C., Nomoto, K., Thielemann, F.-K. 1997, in *Thermonuclear Supernovae*, eds. P. Ruiz-Lapuente, R. Canal, J. Isern, Kluwer Academic Publishers, p. 659

Höflich, P., Wheeler, J.C., Thielemann, F.-K. 1998, ApJ., 495, 617

Hubbard, J. 1959, Phys. Rev. Lett. 3 77

Iwamoto, K., Brachwitz, F., Nomoto, K., Kishimomto, N., Umeda, H., Hix, W.R., Thielemann, F.-K. 1999, ApJ Suppl., 125, 439

Johnson, C.W., Koonin, S.E., Lang, G.H., & Ormand, W.E. 1992, Phys. Rev. Lett., 69, 3157

Khokhlov, A.M. 1991, A&A 245, 114; 245, L25

Khokhlov, A.M. 1995, ApJ 449, 695

Koonin, S.E., Dean, D.J., & Langanke, K. 1997, Phys. Rep. 278, 1

Lang, G.H., Johnson, C.W., Koonin, S.E., Ormand, W.E. 1993, Phys. Rev. C, 48, 1518

Langanke, K., Dean, D. J., Radha, P. B., Alhassid, Y. & Koonin, S. E. 1995, Phys. Rev. C, 52, 718.

Langanke, K., Martinez-Pinedo, G. 1998, Phys. Lett. B 436, 19

Langanke, K., Martinez-Pinedo, G. 1999, Phys. Lett. B 453, 187

Livne, E. 1993, ApJ 406, L17

Martinez-Pinedo, G., Langanke, K., & Dean, D.J. 1999, ApJ, in press

Oda, T., Hino, M., Muto, K., Takahara, M., Sato, K. 1994, At. Data Nucl. Data Tables 56, 231

Nabi, J.U. & Klapdor-Kleingrothaus, H.V., 1999, Eur. Phys. J. A5, 337

Niemeyer J.C., & Hillebrandt W. 1995, ApJ, 452, 769

Niemeyer, J.C., Woosley, S.E. 1997, Ap. J. 475, 740

Niemeyer J.C. 1999, ApJ, in press

Nomoto, K. & Kondo, Y., 1991, ApJ 367, L19

Nomoto, K., Yamaoka, H., Shigeyama, T., Kumagai, S., Tsujimoto, T. 1994, in *Supernovae, Les Houches, Session LIV*, eds. S. Bludman, R. Mochkovitch, J. Zinn-Justin (Elsevier, Amsterdam), p. 199

Nomoto, K. et al., 1997 Nucl. Phys. A621, 467c

Nomoto, K., Iwamoto, K., Kishimoto, N. 1997, Science 276, 1378

Nomoto, K., Thielemann, F.-K., & Yokoi, K. 1984, ApJ 286, 644

Nugent, P., Baron, E., Branch, D., Fisher, A., Hauschmidt, P.H. 1997, Ap. J. 485, 812

Radha, P.B., Dean. D.J., Koonin, S.E. Langanke, K., Vogel, P. 1997, Phys. Rev. C56, 3097

Rudolph, D. et al. 1999, Phys. Rev. Lett. 82, 3763

Stratonovich, R. 1957, Dokl. Akad. Nauk. SSR, 115, 1097

Takahara, M., Nino, M., Oda, T., Muto, K., Wolters, A.A., Claudemans, P.W.M.& Sato, K. 1989, Nucl. Phys. A504, 167

Thielemann, F.-K., Nomoto, K., & Yokoi, K. 1986, A&A 158, 17

Thielemann, F.-K. Nomoto, K., Iwamoto, K., Brachwitz, F. 1997, in *Thermonuclear Supernovae*, eds. P. Ruiz-Lapuente, R. Canal, J. Isern, Kluwer Academic Publishers, p. 485

Vetterli, M.C., et al. 1989, Phys. Rev. C40 559

Wheeler, J.C., Harkness, R.P., Khokhlov, A.M., & Höflich, P. 1995, Phys. Rep., 53, 221

Williams, A.L., et al. 1995, Phys. Rev. C51 1144

Woosley, S.E., Weaver, T.A. 1994, in *Les Houches, Session LIV, Supernovae*, eds. S.R. Bludman, R. Mochkovitch, J. Zinn-Justin, Elsevier Science Publ., p. 63